Composition dependence of field induced anisotropy in ferromagnetic $(Co,Fe)_{89}Zr_7B_4$ and $(Co,Fe)_{88}Zr_7B_4Cu_1$ amorphous and nanocrystalline ribbons

P. R. Ohodnicki,[1,a)] J. Long,[1] D. E. Laughlin,[1] M. E. McHenry,[1] V. Keylin,[2] and J. Huth[2]
[1]*Department of Materials Science and Engineering, Carnegie Mellon University, Pittsburgh, Pennsylvania 15213, USA*
[2]*Magnetics, A Division of Spang & Company, Pittsburgh, Pennsylvania 15238, USA*

(Received 28 July 2008; accepted 2 October 2008; published online 4 December 2008)

The composition dependence of field induced anisotropy K_U of field annealed soft ferromagnetic $(Co_{1-x}Fe_x)_{89}Zr_7B_4$ and $(Co_{1-x}Fe_x)_{88}Zr_7B_4Cu_1$ amorphous and amorphous/nanocrystalline "nanocomposite" melt spun ribbons is investigated. With the exception of the highest Co-containing alloys ($x < \sim 0.10$), the observations are discussed in terms of a superposition of directional pair ordering of Fe,Co atoms and an additional contribution presumably due to the presence of Zr and B in both the field crystallized and field annealed amorphous ribbons. The highest Co-containing alloys ($x < \sim 0.10$) contain multiple nanocrystalline phases (bcc, fcc, and hcp) for which a peak in K_U is observed ($K_U \sim 2000-2500$ J/m^3). In this framework, asymmetry in the compositional dependence of K_U resulting in larger values for Co-rich alloys relative to Fe-rich alloys for both the field crystallized and field annealed amorphous alloys is explained in terms of a strong dependence of the Curie temperature of the amorphous phase on the Co content. © *2008 American Institute of Physics*. [DOI: 10.1063/1.3021141]

I. INTRODUCTION

Magnetic field annealing techniques are often used to tailor the properties of soft magnetic materials by inducing a magnetic anisotropy energy $E_A = K_U \sin^2 \theta$.[1,2] θ is the misorientation angle between the induced easy axis and the magnetization and K_U is a first-order uniaxial anisotropy constant. K_U associated with field induced anisotropies ($\sim 10^1-10^3$ J/m^3) are typically orders of magnitude smaller than the local first-order "crystalline" anisotropy constants ($\sim 10^4-10^5$ J/m^3). However, the rapid spatial fluctuations in the orientation of the local crystalline easy axis result in a dramatic reduction in the effective crystalline magnetic anisotropy in nanocrystalline or amorphous magnets.[3] Engineering of the field induced anisotropy is important for soft ferromagnetic Fe,Co-based amorphous and amorphous/nanocrystalline "nanocomposite" alloys as the induced anisotropies can exceed the effective magnetocrystalline anisotropy.[4] The interplay between long-range coherent induced anisotropies and rapid spatial variations in crystalline anisotropies is discussed in the multiphase random anisotropy model.[5,6]

For inductive applications, amorphous and nanocomposite alloys are produced in ribbons and wound into a toroidal core geometry as illustrated in Fig. 1. The two important directions are specified by the long axis of the ribbon (longitudinal) and the width of the ribbon (transverse). The field is applied in the longitudinal direction during applications. Longitudinal field annealing treatments result in relatively high average permeabilities and a striped remanent domain structure [Fig. 1(b)]. Magnetization occurs through migration of magnetic domain walls and large values of K_U can dominate the effective anisotropy and result in domain wall pinning. To minimize this effect by minimizing the value of K_U, rotating magnetic field annealing techniques can be used.[4]

Transverse field annealing treatments result in relatively low permeabilities, linear *B-H* loops, and a transverse striped remanent domain structure [Fig. 1(b)] such that magnetization occurs primarily through rotational processes. Higher K_U alloys result in lower permeabilities and larger anisotropy fields H_K, which are desirable for applications such as high frequency inductors[7] and current sensors.[8] For transverse field annealed cores, an estimate of K_U can be obtained using the expression $K_U = (H_K M_S)/2$. Recent work has demonstrated that Co-rich nanocomposite alloys can exhibit relatively large values of K_U and low permeabilities ($\mu_r \sim 10^2$) after transverse field annealing processing, making them of great interest for these types of applications.[9,10]

Microstructural or atomic-scale changes responsible for field induced anisotropy are subtle and difficult or impossible to directly measure using standard characterization techniques. Direct identification of the dominant mechanism is notoriously difficult, and most conclusions have been based on comparisons of indirect evidence with predictions of

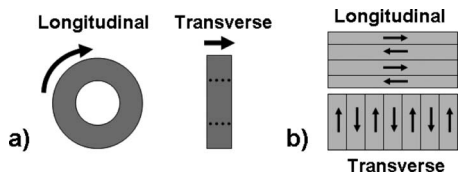

FIG. 1. (a) Toroidal core geometry illustrating the longitudinal and transverse directions. (b) Schematic of domain structure after longitudinal and transverse field annealing.

[a)]Author to whom correspondence should be addressed. Electronic addresses: pohodnic@andrew.cmu.edu and paul.ohodnicki@gmail.com.

models. A particularly successful model is the directional pair ordering model, based on the preferential orientation of pairs of unlike atoms. This model has been used to explain field induced anisotropies measured in binary ferromagnetic crystalline alloys such as Fe–Co[11] and Fe–Ni,[1,2] amorphous ferromagnetic Fe–Co-based and Fe–Ni-based[12,13] alloys, and in the more complex Fe-rich Fe,Co-based nanocomposites.[4] An additional possible source of field induced anisotropy is monatomic directional ordering involving rearrangement of only one type of atom such as interstitial C or N atoms in ferromagnetic crystalline alloys[1,2,14] or metalloid atoms such as B or P in amorphous ferromagnets.[12,13,15] Microstructural origins associated with crystallographic texture,[16] planar defects such as stacking faults,[16–18] or preferential orientation of certain types of local atomic clusters in Co-rich amorphous alloys[19] are examples of other possible sources of induced magnetic anisotropy that have been proposed in the literature.

The nanocomposites are particularly interesting and complex from the standpoint of magnetic field induced anisotropy because of a possible contribution from both the nanocrystalline phases and the intergranular amorphous phase. The directional pair ordering model can rationalize the compositional dependence of K_U in Fe-rich Fe–Co–Zr–B nanocomposites discussed in previous work,[4] but this model is inconsistent with the compositional trend observed for high K_U Co-rich Co–Fe–Zr–Si–B and Co–Fe–Nb–Si–B compositions.[9,10] To better understand the origin of K_U in these complex nanocomposites, we have performed a systematic investigation of the magnitude of K_U as a function of the Fe and Co content in the $(Fe_xCo_{1-x})_{89}Zr_7B_4$ and $(Fe_xCo_{1-x})_{88}Zr_7B_4Cu_1$ alloys. Our composition choice is motivated as follows:

(1) A large body of experimental work has been performed on the technologically relevant Fe-rich and near equiatomic Fe,Co-based alloys of this system.
(2) These alloys do not contain Si, which is known to dissolve into the nanocrystalline phases in high concentrations. This complicates comparison of the compositional dependence of K_U with predictions of theories of field induced anisotropies for binary systems.

II. EXPERIMENTAL PROCEDURE

Fe and Co-based amorphous ribbons of compositions $(Co_{1-x}Fe_x)_{88}Zr_7B_4Cu_1$ and $(Co_{1-x}Fe_x)_{89}Zr_7B_4$ with $0 \leq x \leq 1$ were first synthesized by arc-melting followed by rapid solidification through melt-spinning processing. These ribbons were wound into toroidal cores and annealed for 1 h in a 2 T transverse magnetic field at Magnetics, a division of Spang & Company. A number of different annealing temperatures were chosen to lie significantly below and above the lowest crystallization temperature of these alloys. The magnetic properties and field induced magnetic anisotropy were measured through vibrating sample magnetometry (VSM) and ac permeametry of toroidal tape-wound cores of the synthesized ribbons. The phase identity of the nanocrystals formed during crystallization was investigated using x-ray diffraction (XRD) with a Philips X'pert thin film diffractometer.

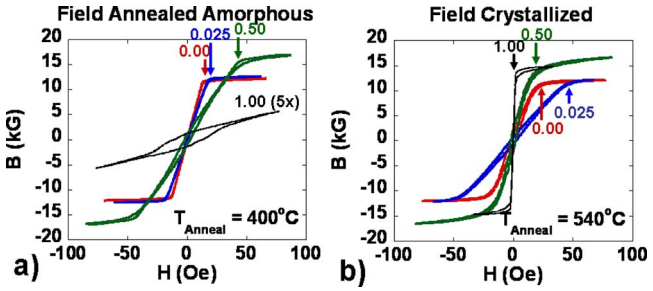

FIG. 2. (Color online) Representative dynamic (f=3 kHz) B-H loops obtained for toroidal cores of $(Fe_xCo_{1-x})_{89}Zr_7B_4$ (Co-rich) and $(Fe_xCo_{1-x})_{88}Zr_7B_4Cu_1$ (Fe-rich and equiatomic) alloys after transverse magnetic field annealing at (a) T_{Anneal}=400 °C and (b) T_{Anneal}=540 °C. The estimated anisotropy field H_K for each B-H loop is indicated by a vertical arrow, and the number listed corresponds to x. For the x=1.00 sample annealed at T_{Anneal}=400 °C, B is multiplied by a factor of 5 for clarity.

III. EXPERIMENTAL RESULTS AND DISCUSSION

In Fig. 2, examples of B-H loops measured after transverse magnetic field annealing at two different temperatures are presented. In Fig. 2(a), T_{Anneal}=400 °C and in Fig. 2(b), T_{Anneal}=540 °C. XRD patterns obtained from the side of the ribbon in contact with the cooling wheel (wheel side) do not provide evidence of a crystalline phase for the as-cast ribbons. While T_{Anneal}=540 °C is sufficiently high to result in partial (primary) crystallization to form a microstructure consisting of a large volume fraction of nanocrystalline phases surrounded by an intergranular amorphous matrix, no evidence for crystalline phase can be found in XRD patterns obtained from the wheel side of the ribbons after the T_{Anneal}=400 °C annealing treatment. Therefore, the former treatment results in field crystallization, while the latter results in field annealing of the amorphous precursor. Consistent with a number of discussions in previous work,[20,21] only evidence of a bcc nanocrystalline phase is observed in obtained XRD data from these alloys as illustrated in Fig. 3 for

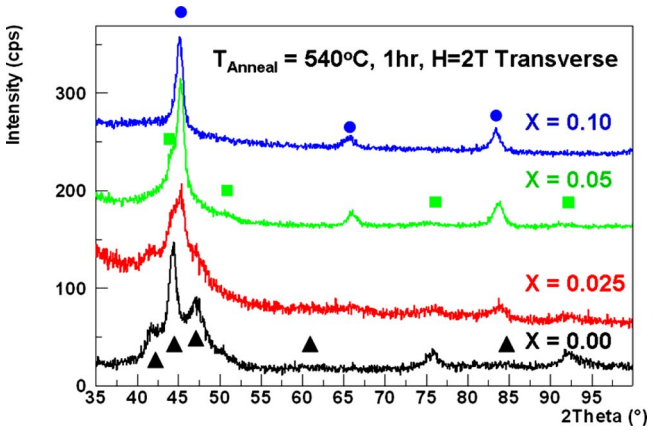

FIG. 3. (Color online) XRD data for transverse magnetic field annealed $(Co_{1-x}Fe_x)_{89}Zr_7B_4$ alloys illustrating only a bcc nanocrystalline phase for all but the highest Co-containing alloys ($x < \sim 0.10$). Circles=peaks indexed to bcc, squares=peaks indexed to fcc, and triangles=peaks indexed to hcp.

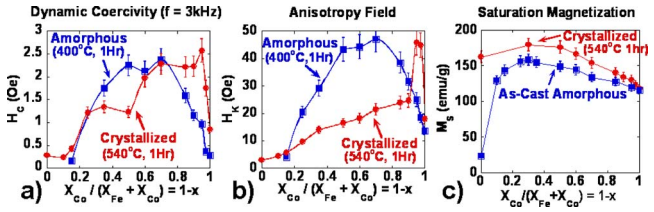

FIG. 4. (Color online) (a) H_C and (b) H_K as functions of composition for the field annealed amorphous (T_{Anneal}=400 °C, squares) and field crystallized (T_{Anneal}=540 °C, circles) toroidal $(Fe_xCo_{1-x})_{89}Zr_7B_4$ (Co-rich) and $(Fe_xCo_{1-x})_{88}Zr_7B_4Cu_1$ (Fe-rich and equiatomic Fe:Co) cores estimated from dynamic *B-H* loops obtained at f=3 kHz as illustrated in Fig. 2. In (c) M_S values estimated independently at room temperature using a VSM (H =5 kOe) are shown for as-cast amorphous and field crystallized (T_{Anneal} =540 °C) alloys.

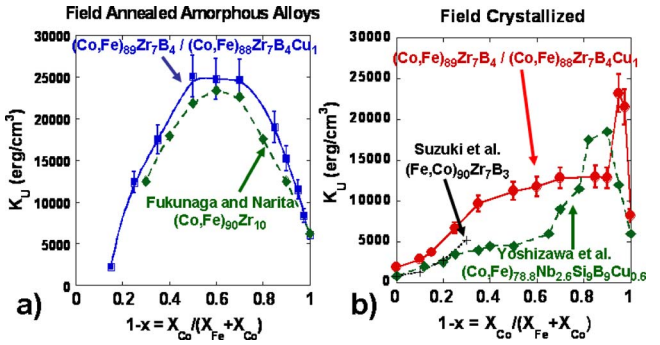

FIG. 5. (Color online) Composition dependences of K_U for (a) field annealed amorphous (T_{Anneal}=400 °C, squares) and (b) field crystallized (T_{Anneal}=540 °C, circles) $(Fe_xCo_{1-x})_{89}Zr_7B_4$ (Co-rich) and $(Fe_xCo_{1-x})_{88}Zr_7B_4Cu_1$ (Fe-rich and equiatomic) toroidal cores estimated from H_K and M_S in Fig. 4. The previous results of field annealed amorphous (a) $(Co,Fe)_{90}Zr_{10}$ alloys, by Fukunaga and Narita (diamonds) (Ref. 13), (b) field crystallized $(Co,Fe)_{78.8}Nb_{2.6}Si_9B_9Cu_{0.6}$, by Yoshizawa *et al.* (Refs. 9 and 10) (diamonds), and (b) field crystallized $(Co,Fe)_{90}Zr_7B_3$ alloys, by Suzuki *et al.* (Ref. 4) (+), are shown for comparison.

T_{Anneal}=540 °C with the exception of the highest Co-containing alloys ($x<\sim 0.10$), for which evidence of both fcc and hcp phases is also found.[22]

Based on the measured *B-H* loops presented in Fig. 2, the estimated values of the anisotropy field H_K and the dynamic coercivity H_C are presented in Figs. 4(a) and 4(b) as functions of composition. H_K was estimated by extrapolation of the lowest field linear portion of the *B-H* loop to the saturation induction (see vertical arrows in Fig. 2). For the highest Fe-containing field annealed amorphous alloys, the *B-H* loop deviates from linearity and requires relatively large fields to saturate [see the x=1.00 alloy in Fig. 2(a) for the most extreme example]. For these alloys, values of H_K could not be extracted and they are not included in the plots below. The estimated values of H_C are sensitive to factors such as strain state, thickness, and overall ribbon quality and can vary significantly for alloys of the same composition, which is responsible for some discrepancies between values reported here and in our previous works.[22,23] However, the estimated values of H_K are more reproducible and relatively insensitive to these factors. The error bars in Figs. 4(a) and 4(b) represent the error in accurately measuring the value for a given sample. Figure 4(a) shows that the highest Co-containing field crystallized ribbons tend to exhibit larger dynamic H_C values than those of the corresponding field annealed amorphous ribbons and the Fe-rich field crystallized ribbons.

The estimated saturation magnetizations at room temperature, M_S, measured independently using a VSM with H =5 kOe of as-cast amorphous ribbons and the transverse field crystallized ribbons (T_{Anneal}=540 °C) are shown in Fig. 4(c). The Fe-rich alloys exhibit higher saturation inductions than those of the Co-based alloys. The drop in M_S for the most Fe-rich amorphous alloys is due to the relatively low Curie temperatures of these alloys.

Based on the values of H_K and M_S in Figs. 4(b) and 4(c), the estimated values of K_U are shown in Figs. 5(a) and 5(b). For comparison, data from a number of previously published works in related alloy systems are also shown including the field crystallized $(Co,Fe)_{78.8}Nb_{2.6}Si_9B_9Cu_{0.6}$ alloys,[9,10] the Fe-rich field crystallized $(Fe,Co)_{90}Zr_7B_3$ alloys,[4] and the field annealed amorphous $(Co,Fe)_{90}Zr_{10}$ alloys (reproduced assuming a density of $\sim$7.8 g/cm^3).[13] Figures 5(a) and 5(b) demonstrate that K_U is significantly larger for the field annealed amorphous alloys than for the field crystallized alloys investigated here over the majority of the composition range. The exceptions are the high Fe-containing alloys ($x>\sim 0.90$) for which accurate estimates of K_U could not be obtained for the field annealed amorphous alloys and the high Co-containing alloys ($x<\sim 0.10$), for which K_U of the field crystallized alloys is larger than that of the field annealed amorphous alloys.

The main features of Figs. 5(a) and 5(b) common to both the field annealed amorphous and field crystallized alloys include:

(1) nonzero K_U for the x=0.00 (Fe-free) and x=1.00 (Co-free) alloys for which directional pair ordering of Fe and Co atoms is not a possible mechanism, and
(2) asymmetric compositional dependences resulting in a tendency for higher field induced anisotropy in the Co-rich alloys.

Further, a peak in K_U is observed for the dilute Fe-containing (x=0.05 and x=0.025) field crystallized alloys in Fig. 5(b), which is similar to observations reported previously.[9,10] However, the high K_U compositions here correspond to higher Co-containing alloys with multiple crystalline phases present after primary crystallization while those investigated by the previous authors[9,10] exhibited only bcc nanocrystalline phase. In the remainder of this section, we discuss potential explanations for observations 1 and 2 in light of the conclusions of previous authors. A detailed discussion of the phase evolution, microstructure, and field induced anisotropy in the Co-rich compositions (x=0.10, 0.05, 0.025, and 0.00) that exhibit a peak in K_U after field crystallization is reserved for a separate publication due to their additional complexity.[24] We note that the large K_U for the x=0.025 and x=0.05 alloys is thought to be associated with the nanocrystalline phases that form upon crystallization.

It was shown that the increase in K_U upon substitution of Co for Fe in Fe-rich field crystallized alloys of composition $(Fe,Co)_{90}Zr_7B_3$ could be well fit by an expression of the form $K_U \approx K_A + K_B[X_{Co}/(X_{Fe}+X_{Co})]^2$.[4] Note that we use the

symbols K_A and K_B here rather than K_0 and K_1 as used by the previous authors[4] to avoid confusion with the standard terms in the phenomenological expansion of the magnetocrystalline anisotropy. The data obtained here are reasonably consistent with the previous work but the estimated values of $K_A \sim 200$ J/m^3 and $K_B \sim 7560$ J/m^3 are significantly larger than the values of $K_A \sim 76$ J/m^3 and $K_B \sim 4900$ J/m^3 reported previously as seen in Fig. 5(b). Based on this form of the compositional dependence, it was concluded that multiple mechanisms of field induced anisotropy must be active and that K_B was attributed to directional pair ordering of Fe and Co atoms in the crystalline phase, while K_A was attributed to the presence of dissolved Zr and B in the crystalline phase. Although not previously discussed, possible mechanisms for the latter contribution include an effective directional pair ordering of substitutionally dissolved Zr and B with the Fe and Co atoms or monatomic directional ordering of interstitially incorporated B. The entire value of K_U was assumed to be due to the crystalline phase because the Curie temperature of the as-cast amorphous ribbons exhibited Curie temperatures well below the field crystallization temperatures.[4]

For the higher Co-containing alloys investigated here, the T_C of the as-cast amorphous ribbons increases dramatically with increasing Co content. Thus, it is reasonable to assume that K_U measured for the Co-rich field crystallized alloys should include a contribution from the intergranular amorphous phase.[4] Therefore, the asymmetric compositional dependence of K_U for the field annealed amorphous alloys of Fig. 5(a) provides a potential explanation for the corresponding asymmetry observed for the field crystallized alloys in Fig. 5(b).

The $(Co_{1-x}Fe_x)_{90}Zr_{10}$ field annealed amorphous alloys studied by Fukunaga and Narita[13] exhibited a similar compositional dependence of K_U as the $(Co_{1-x}Fe_x)_{89}Zr_7B_4$ and $(Co_{1-x}Fe_x)_{88}Zr_7B_4Cu_1$ compositions studied here as shown in Fig. 5(a). The authors demonstrated that this dependence could be explained by a superposition of directional pair ordering of Fe–Co atoms and an additional contribution presumably associated with the presence of Zr. These conclusions were based on fits of the directional pair ordering model to the data in Fig. 5(a) for fcc-based binary ferromagnets with a tendency for chemical segregation after: (1) normalizing by a Curie temperature dependent factor, $g(T_{\text{Anneal}}, T_{\text{Measurement}}, x)$, and (2) subtracting the contribution measured for the Fe-free $Co_{90}Zr_{10}$ alloy assuming that it exhibits the same temperature dependence and is constant across the composition range when normalized by this factor. The assumed form of $g(T_{\text{Anneal}}, T_{\text{Measurement}}, x)$ was

$$g(T_{\text{Anneal}}, T_{\text{Measurement}}, x) = \left[\frac{M_S(T_{\text{Anneal}}, x)}{M_S(0,x)}\right]^2 \left[\frac{M_S(T_{\text{Measurement}}, x)}{M_S(0,x)}\right]^2 = [m(T_{\text{Anneal}}, x)]^2 [m(T_{\text{Measurement}}, x)]^2. \quad (1)$$

In Eq. (1), T_{Anneal} is the field annealing temperature, $T_{\text{Measurement}}$ is the temperature at which the value of K_U is measured after annealing, x is the atomic ratio of Fe to (Fe+Co), M_S is the saturation magnetization, and m is the reduced magnetization at a particular temperature and composition. The asymmetry observed could be completely accounted for by a strong dependence of T_C on the Co content of the amorphous alloy resulting in a higher temperature stability of magnetic properties for Co-rich alloys. Based on the similarity with the compositional trend of K_U measured for the field annealed amorphous alloys investigated here, it is reasonable to assume that the same conclusions hold for the $(Co_{1-x}Fe_x)_{89}Zr_7B_4$ and $(Co_{1-x}Fe_x)_{88}Zr_7B_4Cu_1$ alloys. In addition, the similar magnitudes of K_U for the Fe-free ($x=0.00$) field annealed amorphous $Co_{89}Zr_7B_4$ and $Co_{90}Zr_{10}$ ribbons compared in Fig. 5(a) suggest that a similar mechanism may be responsible for K_U of the Fe-free compositions despite the complete absence of B in the $(Co,Fe)_{90}Zr_{10}$ alloy series.

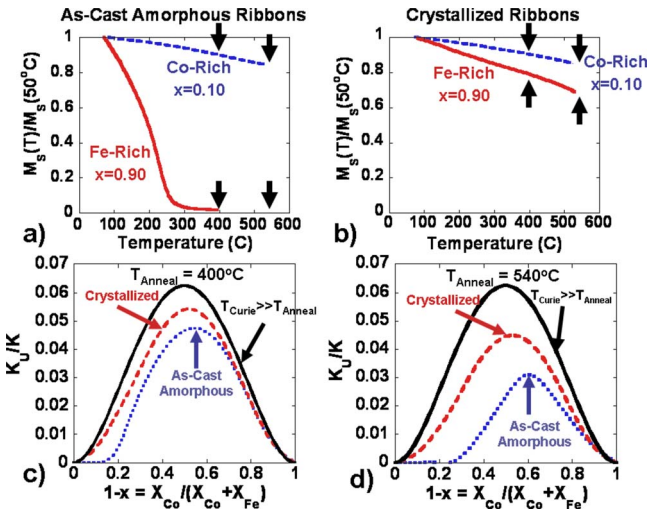

FIG. 6. (Color online) In (a) and (b) the reduced magnetization approximated as $M_S(T)/M_S(50\ ^\circ\text{C})$ for a Co-rich $(Fe_{0.1}Co_{0.9})_{89}Zr_7B_4$ alloy and an Fe-rich $(Fe_{0.9}Co_{0.1})_{88}Zr_7B_4Cu_1$ alloy are shown for as-cast amorphous ribbons on heating (a) and crystallized ribbons on cooling (b) with heating and cooling rates of approximately 4 °C/min. In (c) and (d) the predicted compositional dependence of K_U/K for binary ideal solid solutions is shown using Eq. (2) and reduced magnetization values estimated as indicated by the vertical arrows in (a) and (b) for both amorphous and crystallized alloys at $T_{\text{Anneal}}=400\ ^\circ\text{C}$ (c) and $T_{\text{Anneal}}=540\ ^\circ\text{C}$ (d). The results assuming $T_{\text{Curie}} \gg T_{\text{Anneal}}$ are presented for comparison.

To illustrate the potential effects of the T_C dependence on the Co content in the alloy systems under investigation here, the directional pair ordering theory for an ideal binary *A*-*B* alloy can be used. In this theory, the predicted variation in K_U with the mole fraction of *B*, X_B, follows Eq. (2):[2,12]

$$K_U = K[m(T_{\text{Anneal}}, X_B)]^2 [m(T_{\text{Measurement}}, X_B)]^2 X_B^2 (1 - X_B)^2. \quad (2)$$

In Eq. (2), K is a factor that is independent of composition. A number of magnetization curves were measured as a function of temperature to estimate the values of $[m(T_{\text{Anneal}}, X_B)]^2$ for both the amorphous precursor and the field crystallized ribbons as presented in Figs. 6(a) and 6(b) for alloys of varying Co contents. The values of K_U/K estimated according to Eq. (2) assuming $[m(T_{\text{Measurement}}, X_B)]^2 = 1$, $[m(T_{\text{Anneal}}, X_B)]^2 \approx [M_S(T_{\text{Anneal}}, X_B)/M_S(50\ ^\circ\text{C}, X_B)]^2$, and $X_B = X_{\text{Co}}/(X_{\text{Co}}+X_{\text{Fe}}) = 1-x$ are presented in Figs. 6(c) and 6(d) for both the crystallized and as-cast amorphous ribbons for values of $T_{\text{Anneal}}=400$ and 540 °C. These assumptions are good ap-

proximations for all but the highest Fe-containing amorphous ribbons. For comparison, the predicted compositional dependence is also presented for the limiting case where T_C is much larger than the annealing temperature across the entire composition range.

Based on Figs. 6(c) and 6(d) the compositional dependence of T_C is expected to result in a strongly asymmetric compositional dependence of K_U for the field annealed amorphous alloys, while the effect is less pronounced for crystallized ribbons. Although Eq. (2) assumes only directional pair ordering of Fe and Co atoms, the Curie temperature effect would also apply to contributions associated with the presence of B and Zr including monatomic directional ordering of interstitial B or directional pair ordering of Fe,Co with substitutional B and Zr. For the field crystallized ribbons, the simple expression in Eq. (2) is not strictly valid because of a potential contribution from both the nanocrystalline phases and the intergranular amorphous phase with different effective Curie temperatures. Instead, a better approximation to $K_U(x)$ for field crystallized $(Fe_xCo_{1-x})_{89}Zr_7B_4$ and $(Fe_xCo_{1-x})_{88}Zr_7B_4Cu_1$ alloys is given by Eq. (3):

$$\begin{aligned} K_U(x) &= K_{U\text{Amorphous}}(x) + K_{U\text{Crystalline}}(x) \\ &= V_{\text{Amorphous}} K_{\text{Amorphous}} [m(T_{\text{Anneal}},x)]^2_{\text{Amorphous}} \\ &\quad \times [m(T_{\text{Measurement}},x)]^2_{\text{Amorphous}} f_{\text{Amorphous}}(x) \\ &\quad + (1 - V_{\text{Amorphous}}) K_{\text{Crystalline}} \\ &\quad \times [m(T_{\text{Anneal}},x)]^2_{\text{Crystalline}} \\ &\quad \times [m(T_{\text{Measurement}},x)]^2_{\text{Crystalline}} f_{\text{Crystalline}}(x). \end{aligned} \tag{3}$$

$V_{\text{Amorphous}}$ is the volume fraction of the amorphous phase and $f_{\text{Amorphous}}(x)$ [or $f_{\text{Crystalline}}(x)$] is the function that describes the compositional dependence of $K_{U\text{Amorphous}}$ (or $K_{U\text{Crystalline}}$) assuming that $T_{\text{Curie}} \gg T_{\text{Anneal}}, T_{\text{Measurement}}$. To estimate the potential contribution from each phase to the measured K_U for the field crystallized alloys in Fig. 5(b), the following procedure has been employed:

(1) The measured values of K_U for the field annealed amorphous alloys shown in Fig. 5(a) have been normalized by the following factor at each composition: $[m(540\ ^\circ\text{C},x)]^2/[m(400\ ^\circ\text{C},x)]^2$. The resultant values represent the extrapolated values of K_U of the field annealed amorphous ribbons to $T_{\text{Anneal}}=540\ ^\circ\text{C}$ and are plotted in Fig. 7(a).
(2) Assuming the intergranular amorphous phase exhibits the same compositional dependence of K_U as the corresponding field annealed amorphous ribbons, the resultant values of step 1 were multiplied by an assumed value of $V_{\text{Amorphous}}$ to estimate $K_{U\text{Amorphous}}$ as presented in Fig. 7(b). Values of $V_{\text{Amorphous}}=25\%$ and 40% are used here.
(3) The estimated $K_{U\text{Amorphous}}$ was subtracted from the measured values of K_U for the field crystallized ribbons in Fig. 5(b) to estimate the corresponding values of $K_{U\text{Crystalline}}$ as presented in Fig. 7(b).

With the exception of the high K_U dilute Fe-containing compositions $[1-x=X_{\text{Co}}/(X_{\text{Co}}+X_{\text{Fe}}) > \sim 0.90]$, the asymmetry in the compositional dependence of K_U is reduced in the estimated $K_{U\text{Crystalline}}$ in Fig. 7(b). These results suggest that an increasing contribution from the intergranular amorphous phase for Co-rich alloys could be a major source of the asymmetry in the compositional dependence of K_U for field crystallized alloys. In addition, a local minimum in $K_{U\text{Crystalline}}$ is now observed for compositions with near equiatomic Fe:Co ratios which would be expected to arise due to chemical ordering occurring in the bcc crystalline phase[25,26] as observed in bulk field annealed Fe–Co binary crystalline alloys.[11] Considering the rough estimates of $K_{U\text{Crystalline}}$ and $K_{U\text{Amorphous}}$, no features observed in Fig. 7(b) are clearly inconsistent with a combination of directional pair ordering of Fe and Co atoms with an additional contribution that is presumably due to the B and Zr in the bcc crystalline and amorphous phases for $X_{\text{Co}}/(X_{\text{Co}}+X_{\text{Fe}}) < \sim 0.90$. For the dilute Fe-containing nanocomposites with multiple nanocrystalline phases and large field induced anisotropies, the situation is clearly more complicated.[24]

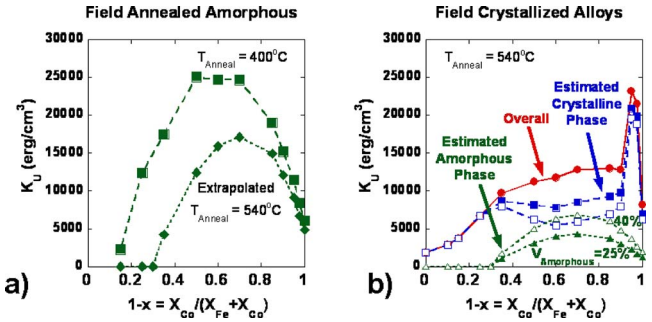

FIG. 7. (Color online) (a) Measured values of K_U for field annealed amorphous alloys of composition $(Co_{1-x}Fe_x)_{89}Zr_7B_4$ at $T_{\text{Anneal}}=400\ ^\circ\text{C}$ (squares) as well as the extrapolated values for $T_{\text{Anneal}}=540\ ^\circ\text{C}$ (diamonds) assuming the annealing temperature dependence follows $[m(T_{\text{Anneal}},x)]^2$. (b) Estimated contributions to K_U (closed circles) from $K_{U\text{Amorphous}}$ (triangles) and $K_{U\text{Crystalline}}$ (squares) for field crystallized alloys at $T_{\text{Anneal}}=540\ ^\circ\text{C}$ by assuming $V_{\text{Amorphous}}=25\%$ (closed symbols) and 40% (open symbols).

The Curie temperature effect for the amorphous phase discussed above is not the only possible source of an asymmetry in the compositional dependences of K_U as a function of x for $(Fe_xCo_{1-x})_{89}Zr_7B_4$ and $(Fe_xCo_{1-x})_{88}Zr_7B_4Cu_1$ alloys. Examples of additional possible sources of asymmetry include:

(1) a stronger interaction responsible for Co–Zr and Co–B directional pair orderings or monatomic directional ordering as compared to Fe–Zr and Fe–B,
(2) an interaction responsible for Fe–Co directional pair ordering that is dependent on composition,
(3) chemical partitioning of Fe,Co during crystallization,[27,28] and
(4) a different mechanism active for Co-rich alloys that is not active for Fe-rich alloys.

In previously published data of K_U for bulk binary Fe–Co crystalline alloys,[11,14] a higher K_U was measured for Co-rich alloys than for corresponding Fe-rich alloys. Unfortunately, the previously published data were not normalized for the Curie temperature effect,[14] so it is not clear if an additional source of asymmetry is present for the bulk crystalline FeCo

alloys that would also be active in $K_{U\text{Crystalline}}$ of the complex nanocomposite alloys investigated here.

IV. CONCLUSIONS

The magnitude of field induced anisotropy in the $(Fe_xCo_{1-x})_{89}Zr_7B_4$ and $(Fe_xCo_{1-x})_{88}Zr_7B_4Cu_1$ alloys has been investigated as a function of the relative amounts of Fe and Co. For both field crystallized and field annealed amorphous ribbons, a superposition of several mechanisms of field induced anisotropy is required to explain the compositional dependence. With the exception of the highest Co-containing field crystallized alloys ($x < \sim 0.10$) with multiple nanocrystalline phases (bcc, fcc, and hcp) for which a peak in K_U is observed ($K_U \sim 2000-2500$ J/m^3), the compositional dependences are discussed by assuming directional pair ordering of Fe and Co atoms and additional contributions presumably due to the presence of Zr and/or B. In this framework, an asymmetry in the compositional dependence of K_U for field annealed amorphous alloys can be rationalized by a strong dependence of the Curie temperature on Co content for the amorphous phase. For the field crystallized alloys, both the crystalline and amorphous phases can potentially contribute to K_U and a compositional asymmetry can result from an increased contribution from the intergranular amorphous phase for the Co-rich alloys due to a strong dependence of T_C on Co content.

ACKNOWLEDGMENTS

P.R.O. acknowledges support from a National Defense Science and Engineering Graduate Research Fellowship throughout the preparation of this manuscript. Funding from the National Science Foundation is also acknowledged (NSF Grant No. DMR-0406220).

[1]S. Chikazumi, *Physics of Ferromagnetism* (Wiley, New York, 1986).
[2]R. C. O'Handley, *Modern Magnetic Materials: Principles and Applications* (Wiley InterScience, New York, 1999).
[3]G. Herzer, IEEE Trans. Magn. **26**, 1397 (1990).
[4]K. Suzuki, N. Ito, J. S. Garitaonandia, and J. D. Cashion, J. Appl. Phys. **99**, 08F114 (2006).
[5]K. Suzuki and G. Herzer, *Advanced Magnetic Nanostructures* (Springer, New York, 2006), pp. 365–401.
[6]K. Suzuki, N. Ito, S. Saranu, U. Herr, A. Michels, and J. S. Garitaonandia, J. Appl. Phys. **103**, 07E730 (2008).
[7]J. McCord and J. Paul, IEEE Trans. Magn. **39**, 2359 (2003).
[8]R. Hasegawa, in *Properties and Applications of Nanocrystalline Alloys from Amorphous Precursors*, NATO Science Series II: Mathematics, Physics & Chemistry Vol. 184, edited by B. Idzikowski, P. Svec, and M. Miglierini (Springer, The Netherlands, 2005), pp. 189–207.
[9]Y. Yoshizawa, S. Fujii, D. H. Ping, M. Ohnuma, and K. Hono, Scr. Mater. **48**, 863 (2003).
[10]S. F. Y. Yoshizawa, D. H. Ping, M. Ohnuma, and K. Hono, Mater. Sci. Eng., A **375–377**, 207 (2004).
[11]T. Iwata, Sci. Rep. Res. Inst. Tohoku Univ. [Med] **A10**, 34 (1958).
[12]F. E. Luborsky, J. Magn. Magn. Mater. **7**, 143 (1978).
[13]H. Fukunaga and K. Narita, Jpn. J. Appl. Phys. **21**, L279 (1982).
[14]J. C. Slonczewski, in *Magnetism*, edited by G. T. Bado and H. Suhl (Academic, New York, 1966), Vol. 1.
[15]P. Allia and F. Vinai, IEEE Trans. Magn. **14**, 1050 (1978).
[16]M. Takahashi and T. Kono, Jpn. J. Appl. Phys. **17**, 361 (1978).
[17]J. Sort, S. Surinach, J. S. Munoz, M. D. Baro, M. Wojcik, E. Jedryka, S. Nadolski, N. Sheludko, and J. Nogues, Phys. Rev. B **68**, 014421 (2003).
[18]L. M. Sandler, Y. V. Naglyuk, I. K. Zasimchuk, and Y. L. Zhibolub, Phys. Met. Metallogr. **53**, 191 (1982).
[19]G. Suran, F. Machizaud, and M. Naili, Phys. Rev. B **47**, 15007 (1993).
[20]M. Willard, T. Heil, and R. Goswami, Metall. Mater. Trans. A **38**, 725 (2007).
[21]P. R. Ohodnicki, S. Y. Park, H. K. McWilliams, K. Ramos, D. E. Laughlin, and M. E. McHenry, J. Appl. Phys. **101**, 09N108 (2007).
[22]P. R. Ohodnicki, V. Keylin, H. K. McWilliams, D. E. Laughlin, and M. E. McHenry, J. Appl. Phys. **103**, 07E740 (2008).
[23]P. R. Ohodnicki, S. Y. Park, D. E. Laughlin, M. E. McHenry, V. Keylin, and M. A. Willard, J. Appl. Phys. **103**, 07E729 (2008).
[24]P. R. Ohodnicki, PhD thesis, Carnegie Mellon University, 2008.
[25]M. A. Willard, M. E. McHenry and D. E. Laughlin, Prog. Mater. Sci. **44**, 291 (1999).
[26]M. A. Willard, D. E. Laughlin, and M. E. McHenry, J. Appl. Phys. **87**, 7091 (2000).
[27]D. H. Ping, Y. Q. Wu, K. Hono, M. A. Willard, M. E. McHenry, and D. E. Laughline, Scr. Mater. **45**, 781 (2001).
[28]P. R. Ohodnicki, Jr., Y. L. Qin, D. E. Laughlin, M. E. McHenry, M. Kodzuka, T. Ohkubo, K. Hono, and M. A. Willard, Acta Mater. **57**, 87–96 (2009)